Original Article

Journal of LOW FREQUENCY NOISE, VIBRATION AND ACTIVE CONTROL

Journal of Low Frequency Noise, Vibration and Active Control
0(0) 1–15

DOI: 10.1177/1461348419897644
journals.sagepub.com/home/lfn
SAGE

Physical configuration-based feedforward active noise control using adaptive second-order truncated Volterra filter

Tongrui Peng[1], Quanmin Zhu[1], MO Tokhi[2] and Yufeng Yao[1]

Abstract

This paper presents a physical configuration-based feedforward active noise control scheme with an adaptive second-order truncated Volterra filter for point source cancellation in three-dimensional free-field acoustic environment. The inertial particle swarm optimization (PSO) algorithm is used as the parameter adjustment mechanism for tuning the coefficients of the adaptive Volterra filter. The first motivation of this paper is to provide a precise description of the relationship between the degree of cancellation and the physical distances between system components. The second motivation is to improve the cancellation performance in the presence of nonlinearities with the adaptive Volterra filter in light of the characteristics of sensing microphone and actuating loudspeaker. The reason for choosing the inertial PSO algorithm is that it can avoid the trap of local optima. The work thus presented makes two main contributions. The first is using the degree of cancellation as a function of the physical distances between system components to provide a quantitative analysis of system performance. The second is the application of the adaptive Volterra filter, which achieves improvements in the cancellation performance of the system under different physical configurations with a reasonable compromise with complexity. For consistency with the numerical analysis, several simulation experiments are conducted using MATLAB/Simulink.

Keywords

Physical configuration, second-order truncated Volterra filter, particle swarm optimization

Introduction

Background and literature review

In recent years, extensive acoustic noise is becoming a challenging issue, while its negative effects severely affect people's daily life from both physical and psychological aspects;[1,2] therefore, the control of noise is an important area of research and development. Currently, in terms of simplicity, the source-transmission path-receiver model is widely used for describing the physical process of noise propagation in the medium,[3] and it reveals three opportunities to attenuate the noise level, namely, at the source, at the propagation path and at the receiver point. As for the control approach, passive approach and active approach are the two main approaches. The passive control approach uses absorbers or barriers to attenuate the noise level, which transforms the acoustic energy to heat energy, and it has already demonstrated superior performance in high-frequency noise reduction.[4–6] However, for low-frequency noise, the passive approach is expensive and inconvenient, as increasing acoustic noise wavelength requires a larger size absorbing or damping material. To attenuate low-frequency noise, the active noise control (ANC) method, which is essentially based on the principle of superposition, is proposed.

[1]Faculty of Environment and Technology, Department of Engineering Design and Mathematics, University of the West of England, Bristol, UK
[2]School of Engineering, London South Bank University, London, UK

Corresponding author:
Quanmin Zhu, Faculty of Environment and Technology, Department of Engineering Design and Mathematics, University of the West of England, Bristol, UK.
Email: Quan.Zhu@uwe.ac.uk

The history of ANC can date back to the early 1930s when Lueg first used a loudspeaker to generate the anti-noise to realize the ANC technique.[7] Following Lueg's work, many researchers have devoted their contributions to the development of ANC, and a summary of their contributions can be found in several review papers.[1,2,4,5] In spite of the rapid development of ANC systems, there are still several problems while designing and implementing an ANC system, for example, geometrical design constraints, the usefulness of signal processing algorithms and economical considerations.[2]

For a point source in the free-field acoustical environment, according to the inverse square law, the sound intensity and the sound pressure are inversely proportional to the transmitting distance. Besides, the transmitting distance and the property of the propagation medium determine the sound velocity. In order to describe the physical process of ANC, in 1987, Leitch and Tokhi[1] proposed the geometrical factors-based ANC structure and a transfer function of the controller for presenting the geometric description of the process of cancellation for a compact (point) source in three-dimensional linear (nondispersive) propagation medium (free-field).[1,8] The concept of field cancellation factor is defined in the frequency domain to quantitatively analyse the effect of physical separations of system components on the cancellation performance in decibel (dB), and they presented the critical physical configuration requiring the controller to have infinite gain. Later, a series of related works were published based on this scheme.[9–11] Besides, other researchers also did several works investigating the optimal geometrical configuration of the ANC system. For example, in 1997 and 1998, Martin and Roure[12,13] applied the method of spherical harmonic expansion and genetic algorithms (GAs) on exploring the optimal configuration including number and location of actuators and error sensors, respectively, for the dipole source as the primary source in free-field acoustic environment. In contrast to Leitch and Tokhi's[1] work, Martin and Roure's work is to find the optimal configuration of control sources and error sensor for the minimum squared pressure of the error signal. Duke et al.[14] have used the GA to optimize the control source locations in free-field, and they concluded that the linear arrangement is the best. Several other researchers have focused on exploring the optimal location of secondary sources or transducers in enclosed sound fields, and related summary can be found in several review papers.[15]

In practice, noise sources and the surrounding environment are changing with time, which causes frequency, amplitude, phase and sound velocity of noise sources nonstationary.[5,16] However, the cancellation performance of the ANC system greatly depends on the accuracy of amplitude and phase of the anti-noise generated by a signal processing algorithm.[2] Therefore, the concept of adaptive control is introduced into the ANC system. There are two main components in adaptive control: an adaptive filter and a parameter adjustment mechanism. In linear ANC systems, researchers prefer to choose the finite impulse response (FIR) filter as the adaptive filter and the filtered-x least mean square (FxLMS) algorithm as the parameter adjustment algorithm. However, nonlinearity is a challenging problem for linear ANC systems and mainly from three sources: transducers (e.g. loudspeakers, microphones and actuators), the reference noise and the propagation path, including the primary path, from the reference microphone to the error microphone, and the secondary path, from the loudspeaker to the error microphone.[16–18] To improve the degree of cancellation in the presence of nonlinearities, researchers have proposed several nonlinear adaptive structures and nonlinear adaptive algorithms. For nonlinear structure, the most popular and widely used method is the Volterra series which was proposed by the Italian mathematician Vito Volterra.[19]In 1997, Tan and Jiang[20] used the second-order truncated Volterra (SOV) series as the adaptive filter, and their simulation results demonstrated that the filtered-x second-order Volterra adaptive algorithm performs better than the standard FxLMS algorithm when there is a quadratic nonlinearity in the primary path.[20] In 2001, they expanded their work to propose the general Volterra FxLMS algorithm for a multichannel ANC structure.[21] Their target was to improve the performance in the presence of nonlinearities from the primary source or the secondary path, which might have a nonminimum phase characteristic. In 2004, Carini and Sicuranza proposed the filtered-x affine projection (AP) algorithm for tuning the coefficients of the Volterra filter, and they stated that the AP algorithm has better tractability and convergence compared to conventional FxLMS algorithm with limited increase in complexity.[22]

The population-based optimization algorithms have been proposed for parameter tuning of nonlinear algorithms in recent years and have attracted tremendous attention of researchers worldwide.[23] Population-based optimization algorithm can be divided into two categories, namely, the evolutionary computing-based algorithms and the swarm intelligence-based algorithms. For a nonlinear ANC system, the GA is the most popular and widely used evolutionary computing-based algorithm. For example, in 1999, Yim et al.[24] applied the GA for tuning the coefficients of an adaptive infinite impulse response controller, and in 2007, Russo and Sicuranza[25] applied the GA on Volterra filter-based nonlinear ANC system to compare the performance of the GA algorithm and the conventional FxLMS algorithm. In recent years, the particle swarm optimization (PSO) algorithm, a

representative of the swarm intelligence-based algorithm which was first proposed by Eberhart and Kennedy in 1995,[26] has become popular and has a better convergence speed compared to the GA algorithm. Related works about the application of PSO on the ANC system are not extensive, and the most popular work is done by Rout et al.,[27] where they developed a systematic algorithm for PSO-based ANC system which does not require the identification of the secondary path.

The motivation of this paper

In the authors' previous published paper,[28] based on Leitch and Tokhi's[1] work, a physical configuration-based feedforward ANC structure with an adaptive FIR filter was first proposed to reflect the physical process of cancellation for a point source in a three-dimensional linear propagation medium. The Takagi–Sugeon–Kang fuzzy logic control was used within an adaptive control framework. Later, the inertia weight PSO algorithm was first used to tune the coefficients of the adaptive FIR filter in the author's another subsequent work. The reason for choosing the inertia weight PSO algorithm is that it does not require accurate estimation of the secondary path and gradient information and thus avoids the problem of getting trapped at local minima.[27] Moreover, it converges quickly compared to GA.[27,29] However, a quantitative analysis of the relationship between different distance ratios and the cancellation performance for a point source in the free-field is lacking. Meanwhile, the FIR filter is a linear filter, and its performance in noise cancellation is not good especially for broadband noise.

In light of the above, this paper focuses on the concept of field cancellation factor, defined in the frequency domain, to present the cancellation performance as a function of the distance ratio and to discuss the related physical constraints, providing general suggestions for specific requirements of cancellation in real settings. To address the nonlinearity issue, the SOV filter is used to replace the FIR filter, and detailed discussions are presented in the paper.

Contributions of this paper

There are three contributions to knowledge in this paper:

- The mathematical formulation of the field cancellation factor presented in the paper reveals the effect of distance ratios and coefficients of adaptive filter on the degree of cancellation achieved. It dynamically reflects the effect of different geometrical configurations on the cancellation performance from the perspective of a real physical process.
- The geometrical design of the system and associated physical constraints are provided, and these are deducing from the perspective of scalar values, which supplement the theory of geometric description of the process of cancellation for point sources in three-dimensional linear propagation (free-field).
- The SOV filter is employed in this work, which improves the cancellation performance with a reasonable sacrifice of complexity.

Paper organization

The rest of paper is organized as follows. The next section provides a detailed description of the proposed adaptive second-order Volterra filter-based ANC system with consideration of physical configuration for point source cancellation in a three-dimensional linear propagation medium (free-field). A new concept of field cancellation factor is introduced to present the relationship between the distance ratio and the degree of cancellation, and a series of physical geometry constraints related to separations between system components are provided. Discrete Lyapunov function is used for validating the stability of the proposed ANC system. Next, the process of applying the inertial weight PSO algorithm on the feedforward ANC system is presented. The following section presents several simulation results to verify the cancellation capability of the proposed adaptive ANC system, compare the cancellation performance for both narrowband and broadband noise under different distance ratios and compare the cancellation performance of Volterra filter-based ANC system and FIR filter-based ANC system. The final section concludes the paper.

System description

Figure 1 shows a schematic diagram of single-channel physical configuration-based feedforward ANC structure with an adaptive SOV filter for point source[30] cancellation in three-dimensional free-field acoustic environment.

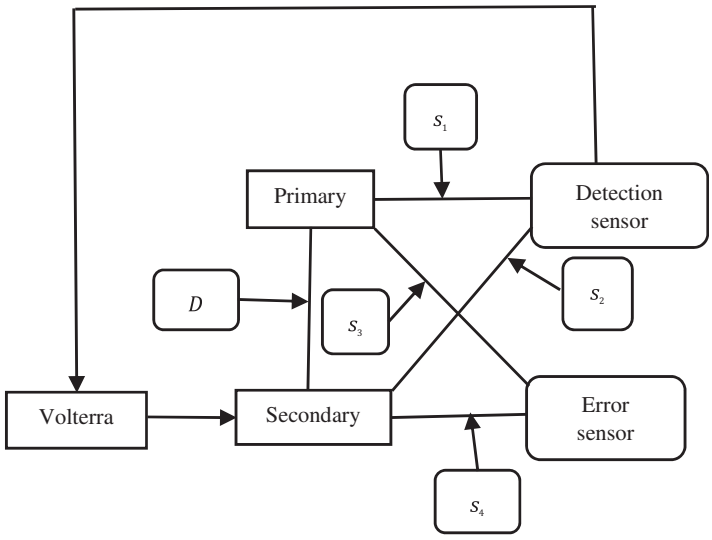

Figure 1. Schematic diagram of geometrical layout of single channel feedforward ANC system.[28]

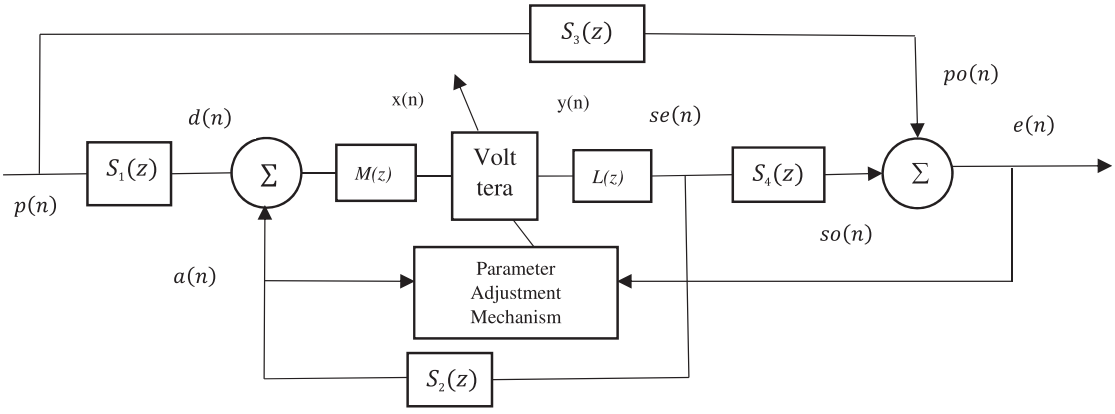

Figure 2. Block diagram of single-channel feedforward ANC system.

The point source generates the primary (unwanted) acoustic wave and emits it into the medium. The detection sensor, placed upstream of the secondary source of a propagating wave,[31] is used for detecting the noise and feeding to the SOV filter for processing. The distances from the detector to the two sources are s_1 and s_2, respectively. The output of the filter transits to the loudspeaker, to generate the secondary (anti-noise) acoustic wave. The secondary acoustic wave is superimposed on the primary acoustic wave at the error sensor, placed downstream of the secondary source and at distances s_3 and s_4 relative to the primary source and the secondary source, respectively. The function of the error sensor is to monitor the cancellation performance of the system.

In terms of analysing conveniently, Figure 2 presents an equivalent block diagram of the single-channel feedforward ANC system. The block diagram contains two feedback loops: one feedback loop is the acoustic feedback, the generated secondary acoustic wave detected by the detection sensor, and another one is parameter adjustment loop, aimed at tuning parameters of the adaptive filter to minimize the pressure amplitude of the error electrical signal.[32]

where $S_1(z)$, $S_2(z)$, $S_3(z)$ and $S_4(z)$ are transfer functions of the acoustic paths s_1, s_2, s_3 and s_4, respectively. $M(z)$ and $L(z)$ are transfer functions of microphone (detection sensor) and loudspeaker, respectively, and detailed descriptions are provided later in the simulations.

The radially acoustic pressure p in the three-dimensional space can be written as a function of the distance r as:[31]

$$p(r) = \frac{j\omega\rho q}{4\pi r} e^{-jkr} \tag{1}$$

where q is the volume velocity, ω is the angular frequency, ρ is the density of the ambient fluid and k is the wave number. It follows that:

$$k = \frac{\omega}{c} \tag{2}$$

where c is the sound speed, determined by:[3]

$$c = \sqrt{\frac{\gamma P}{\rho}} \tag{3}$$

where γ is a constant for particular gas (normally 1.4 for air) and P represents atmospheric pressure. In this study, airborne sound is used and the reason is that air is a nondispersive (linear) medium.

According to equation (1), one can find that the acoustic pressure is decreasing with the increment of distance. In terms of reflecting the geometric spreading of sound during the propagation medium, $S_1(z)$, $S_2(z)$, $S_3(z)$ and $S_4(z)$ are expressed as:

$$S_i(z) = \frac{constant}{s_i} e^{-\frac{\ln Z}{T} t_i} = \frac{constant}{s_i} e^{-F_s \ln Z t_i}, \quad \text{where} \quad i = 1, 2, 3 \text{ and } 4 \tag{4}$$

$$t_i = \frac{s_i}{c}, \quad \text{where} \quad i = 1, 2, 3 \text{ and } 4 \tag{5}$$

where T denotes the sampling interval, and F_s denotes the sampling frequency.

The concept of field cancellation factor[a] is introduced as:

$$K = \frac{GPO(\omega T) - GEO(\omega T)}{GPO(\omega T)} \tag{6}$$

where $GPO(\omega T)$ and $GEO(\omega T)$ represent auto-correlation power spectral density[b] of the primary signal at the receiver point $po(n)$ and the error electrical signal $e(n)$, respectively, one can obtain that:

$$GPO(\omega T) = \left(PO(e^{j\omega T}) \right)^2 \tag{7}$$

$$GEO(\omega T) = \left(E(e^{j\omega T}) \right)^2 \tag{8}$$

Applying the relationship between z transform and discrete-time Fourier transform, equation (6) can be re-written as:

$$K = \frac{\left(PO(Z) \right)^2 - \left(E(Z) \right)^2}{\left(PO(Z) \right)^2} \tag{9}$$

where $PO(Z)$ and $E(Z)$ can be expressed as:

$$PO(z) = S_3(z) P(z) \tag{10}$$

$$E(z) = PO(z) + SO(z) = S_3(z) P(z) + S_4(z) SE(z) \tag{11}$$

Applying equations (10) and (11) to equation (9), we get:

$$K = -2 \frac{S_4(z) SE(z)}{S_3(z) P(z)} - \left(\frac{S_4(z) SE(z)}{S_3(z) P(z)} \right)^2 \tag{12}$$

$SE(z)$ is the transfer function of the secondary source $se(n)$ generated by the loudspeaker and the expression can be stated as:

$$SE(z) = M(z)L(z)W(z)(D(z) + A(z)) \tag{13}$$

where $D(z)$ and $A(z)$ are transfer functions of the detected primary acoustic signal and the acoustic feedback signal. These can be expressed as:

$$D(z) = S_1(z)P(z) \tag{14}$$

$$A(z) = S_2(z)SE(z) \tag{15}$$

The proposed ANC system is a discrete, causal and time-invariant nonlinear system, and the input–output relationship is used here to describe the SOV filter in the time domain as:

$$y(n) = \sum_{i=0}^{N-1} w_1(i)x(n-i) + \sum_{i=0}^{N-1}\sum_{j=i}^{N-1} w_2(i,j)x(n-i)x(n-j) \tag{16}$$

where $x(n)$ and $y(n)$ represent the input and the output signals of the SOV, and in this case, the combination of the primary signal and the acoustical feedback signal is used as the input for the SOV. $w_1(i)$ and $w_2(i,j)$ represent the linear and quadratic kernel functions, and N denotes the length of memory. Consider the definition of causality, both kernel functions must satisfy the requirements as:

$$\begin{cases} w_1(i) = 0, & \text{for } i < 0 \\ w_2(i,j) = 0, & \text{for } i,j < 0 \end{cases} \tag{17}$$

Equation (16) is expanded as:

$$X(n) = (x(n), \cdots, x(n-N+1), x(n)x(n), \cdots, x(n-N+1)x(n-N+1)) \tag{18}$$

$$w(n) = (w_1(0), \cdots, w_1(N), w_2(0,0), \cdots, w_2(N,N)) \tag{19}$$

where the length of the coefficient vector is $\frac{N(N+3)}{2}$.

According to equations (18) and (19), one can find that the number of coefficients of the SOV is larger compared to the FIR filter under the condition of same memory length. These can be re-written as:

$$\begin{aligned} X(n) = (&x(n), \cdots, x(n-N+1), x(n)x(n), \cdots, x(n-N+1)x(n-N+1), \\ &x(n)x(n-1), \cdots, x(n-N+2)x(n-N+1), \cdots, x(n)x(n-N+1)) \end{aligned} \tag{20}$$

$$w(n) = \Big(w_1(0), \cdots, w_1(N), w_2(0,0), \cdots, w_2(N,N), w_2(0,1), \cdots, w_2(N-1,N), \cdots, w_2(0,N)\Big) \tag{21}$$

Re-writing equation (16) as:

$$y(n) = \sum_{v=0}^{N-1} w_1(v)x(n-v) + \sum_{v=0}^{N-1} w_{2,0}(i,j)x(n-v)x(n-v) + \cdots + w_{2,N-1}(i,j)x(n)x(n-N+1) \tag{22}$$

and applying Z-transformation yields:[20]

$$Y(z) = W_1(z)X_1(z) + \sum_{m=0}^{N-1} W_{2,m}(z)X_{2,m}(z) \tag{23}$$

where $W(z) = [W_1(z), \sum_{m=0}^{N-1} W_{2,m}(z)]$. The SOV can be transformed to a multiple channel FIR filter, allowing better description of the concept.

Using equations (14), (15) and (23) with equation (13), yields:

$$SE(z) = \frac{M(z)L(z)W(z)S_1(z)P(z)}{1 - M(z)L(z)W(z)S_2(z)} \tag{24}$$

Substituting for SE(z) from equation (24) into equation (9) yields:

$$K = 2\frac{S_4(z)}{S_3(z)}\frac{S_1(z)}{S_2(z)}\frac{1}{1-\frac{1}{M(z)L(z)W(z)S_2(z)}} - \left(\frac{S_4(z)}{S_3(z)}\frac{S_1(z)}{S_2(z)}\frac{1}{1-\frac{1}{M(z)L(z)W(z)S_2(z)}}\right)^2 \tag{25}$$

where K is expressed in complex frequency domain, and one can find that the value of K depends on three things: physical distance ratios, coefficients of the adaptive filter and physical distance s_2. Coefficients of the adaptive filter are determined by the parameter adjustment mechanism, and this will be described in a later section.

Physical distance constraints

The physical distance between any two points in the three-dimensional plane is a scalar value, and different physical distances account to different configurations of transducers. Considering equation (1), one can find that different physical distances will have a significant effect on the cancellation performance. With reference to equations (4) and (5), the real parts of the complex forms are used for the discussion here, while $|\frac{S_4(z)}{S_3(z)}\frac{S_1(z)}{S_2(z)}|$ can be replaced by $|\frac{s_3}{s_4}/\frac{s_1}{s_2}|$, where $|s_1|$, $|s_2|$, $|s_3|$ and $|s_4|$ are scalar values.

First, the system must satisfy the requirement of cancelling broadband random noise when the acoustic delay is larger than the electrical delay.[5] It follows that:

$$|s_3| > |s_1| + |s_4| \tag{26}$$

Thus, according to the relationship between the geometric mean and arithmetic mean, it follows that:

$$|s_3| > |s_1| + |s_4| \geq 2\sqrt{|s_1 s_4|} \tag{27}$$

where only $|s_1| = |s_4|$, then the notation = exist.

Based on the property of inequality, multiplication, it follows that:

$$|s_3 s_2| > 2|s_2|\sqrt{|s_1 s_4|} \tag{28}$$

Applying equation (26) to $|\frac{s_3 s_2}{s_4 s_1}|$, one can obtain that:

$$\left|\frac{s_3 s_2}{s_4 s_1}\right| > \frac{2|s_2|\sqrt{|s_1 s_4|}}{|s_4 s_1|} = \frac{2|s_2|}{\sqrt{|s_1 s_4|}} \tag{29}$$

Equation (29) defines the main principle of physical constraints, and the cases given in the sections below are discussed.

$|\frac{s_3}{s_4}/\frac{s_1}{s_2}| > 1$. In this condition, only the condition of $|s_1| > |s_2|$ is considered. Combining equation (29) and $|\frac{s_3}{s_4}/\frac{s_1}{s_2}| > 1$, one can find that it is necessary to compare the values of $\frac{2|s_2|}{\sqrt{|s_1 s_4|}}$ and 1. For the case of $\frac{2|s_2|}{\sqrt{|s_1 s_4|}} \geq 1$, it follows that:

$$\frac{2|s_2|}{\sqrt{|s_1 s_4|}} \geq 1 \Rightarrow |s_2| \geq \frac{\sqrt{|s_1 s_4|}}{2} \tag{30}$$

where considering that $|s_1| > |s_2|$, it follows that:

$$|s_1| > |s_2| > \frac{\sqrt{|s_1 s_4|}}{2} \Rightarrow 4|s_1| > |s_4| \tag{31}$$

For the case of $\frac{2|s_2|}{\sqrt{|s_1 s_4|}} < 1$, one can obtain that:

$$\frac{2|s_2|}{\sqrt{|s_1 s_4|}} < 1 \Rightarrow |s_2| < \frac{\sqrt{|s_1 s_4|}}{2} \tag{32}$$

where $|s_1| > |s_2|$, and thus comparing $|s_1|$ and $\frac{\sqrt{|s_1 s_4|}}{2}$, one can obtain the constraints as follows:

$$\begin{cases} |s_2| \le \dfrac{\sqrt{|s_1 s_4|}}{2}, & \text{when } 4|s_1| \ge |s_4| \\ |s_2| < |s_1|, & \text{when } 4|s_1| < |s_4| \end{cases} \tag{33}$$

$|\frac{s_3}{s_4} / \frac{s_1}{s_2}| = 1$. Combining equation (29) and condition $|\frac{s_3}{s_4} / \frac{s_1}{s_2}| = 1$, one can obtain that:

$$|s_1 s_4| = |s_2 s_3| > 2|s_2|\sqrt{|s_1 s_4|} \Rightarrow |s_2| < \frac{\sqrt{|s_1 s_4|}}{2} \tag{34}$$

where, after considering the condition $s_1 > s_2$, one can obtain:

$$\begin{cases} |s_2| < \dfrac{\sqrt{|s_1 s_4|}}{2}, & \text{when } 4|s_1| \ge |s_4| \\ |s_2| < |s_1|, & \text{when } 4|s_1| < |s_4| \end{cases} \tag{35}$$

$|\frac{s_3}{s_4} / \frac{s_1}{s_2}| < 1$. Considering equation (29) and condition $|\frac{s_3}{s_4} / \frac{s_1}{s_2}| < 1$, one can obtain that:

$$|s_1 s_4| = |s_2 s_3| > 2|s_2|\sqrt{|s_1 s_4|} \Rightarrow |s_2| < \frac{\sqrt{|s_1 s_4|}}{2} \tag{36}$$

where the results are same as in equation (35).

The physical distance constraints can thus be summarized as follows:

$$\begin{aligned} \left|\frac{s_3}{s_4} \Big/ \frac{s_1}{s_2}\right| > 1 \begin{cases} |s_1| < |s_2|, & \text{no specific requirments} \\ |s_1| > |s_2|, & \begin{cases} \dfrac{2|s_2|}{\sqrt{|s_1 s_4|}} \ge 1, & 4|s_1| > |s_4| \\ \dfrac{2|s_2|}{\sqrt{|s_1 s_4|}} < 1, & \begin{cases} |s_2| \le \dfrac{\sqrt{|s_1 s_4|}}{2}, & \text{when } 4|s_1| \ge |s_4| \\ |s_2| < |s_1|, & \text{when } 4|s_1| < |s_4| \end{cases} \end{cases} \end{cases} \\ \left|\frac{s_3}{s_4} \Big/ \frac{s_1}{s_2}\right| = 1, |s_1| > |s_2|, \begin{cases} |s_2| < \dfrac{\sqrt{|s_1 s_4|}}{2}, & \text{when } 4|s_1| \ge |s_4| \\ |s_2| < |s_1|, & \text{when } 4|s_1| < |s_4| \end{cases} \\ \left|\frac{s_3}{s_4} \Big/ \frac{s_1}{s_2}\right| < 1, |s_1| > |s_2|, \begin{cases} |s_2| < \dfrac{\sqrt{|s_1 s_4|}}{2}, & \text{when } 4|s_1| \ge |s_4| \\ |s_2| < |s_1|, & \text{when } 4|s_1| < |s_4| \end{cases} \end{aligned} \tag{37}$$

Stability of the proposed feedforward ANC system

Inspired by previous literature,[33] the discrete-type Lyapunov stability theory is used for exploring the system stability. The discrete Lyapunov function is defined as:

$$V(n) = \frac{1}{2}(e(n))^2 \tag{38}$$

The change of Lyapunov function is:

$$\Delta V(n) = \frac{1}{2}(e(n+1)^2 - e(n)^2) \tag{39}$$

where $e(n+1)$ can be expressed in terms of the error electrical signal $e(n)$ and the change of error electrical signal $\Delta e(n)$:

$$\Delta e(n) = e(n+1) - e(n) \tag{40}$$

A general stability theorem can be stated as follows.

Theorem. Notation s_1, s_2, s_3 and s_4 represent four physical distances in the ANC system. If the distance ratio $|\frac{s_3 s_2}{s_4 s_1}|$ is smaller than $|1 - \frac{1}{|MLS_2W|}|$, then the local stability of the proposed adaptive ANC system can be guaranteed.

Proof. The error electrical signal $e(n)$ can be expressed in terms of primary signal $p(n)$:

$$e(n) = p(n)\left(S_3 + S_4 \frac{MLS_1W}{1 - MLS_2W}\right) \tag{41}$$

Then, the change of the error electrical signal $\Delta e(n)$ can be obtained as:

$$\Delta e(n) = S_3 + S_4 \frac{MLS_1W}{1 - MLS_2W} \tag{42}$$

$$\begin{aligned} \Delta V(n) &= e(n)\Delta e(n) + \frac{1}{2}(\Delta e(n))^2 = \Delta e(n)\left(e(n) + \frac{1}{2}\Delta e(n)\right) \\ &= \frac{S_3\Big(1 + 2p(n)\Big) + (S_4S_1 - S_2S_3)MLW + 2(S_4S_1 - S_2S_3)MLWp(n)}{(1 - MLS_2W)^2} \end{aligned} \tag{43}$$

In order to make $\Delta V(n) < 0$, one can obtain that:

$$S_3\Big(1 + 2p(n)\Big) + (S_4S_1 - S_2S_3)MLW + 2(S_4S_1 - S_2S_3)MLWp(n) < 0 \tag{44}$$

Then,

$$(S_4S_1 - S_2S_3)MLW + S_3 < 0 \tag{45}$$

After combining and simplifying, one can obtain that:

$$\left|\frac{S_4}{S_3}\frac{S_1}{S_2}\right| < \left|1 - \frac{1}{|MLS_2W|}\right| \tag{46}$$

As discussed above, $|\frac{S_4}{S_3}\frac{S_1}{S_2}|$ equals to $|\frac{s_3 s_2}{s_4 s_1}|$ and equation (46) can be re-written as:

$$\left|\frac{s_3 s_2}{s_4 s_1}\right| < \left|1 - \frac{1}{|MLS_2W|}\right| \tag{47}$$

Therefore, if distance ratios and coefficient values satisfy equation (47) and $\Delta V(n) < 0$, the system is locally stable.

Inertia weight PSO algorithm

The ANC system aims to reduce the pressure amplitude of the error signal at the receiver point, and the degree of cancellation depends on the efficiency of the parameter adjustment mechanism. In this case, consider equations (20) to (22), the second-order Volterra filter can be expressed in the form of a multichannel FIR filter, then the form of the coefficients is assumed as:[27]

$$w = \begin{bmatrix} w_1^1 & w_1^2 & \cdots & w_1^D \\ w_2^1 & w_2^2 & \cdots & w_2^D \\ \cdots & \cdots & \cdots & \cdots \\ w_N^1 & w_N^2 & \cdots & w_N^D \end{bmatrix} \tag{48}$$

where the coefficient vector is an $N\ D$ matrix. The symbol N represents the size of the dimensional search space, and the symbol D denotes the number of particles in the dimensional search space. Each column of the matrix represents the coefficient value of an adaptive filter in the filter bank, and the relationship between the N and D in this case is:

$$D = N + 1 \tag{49}$$

The mains steps of the inertial PSO algorithm can be explored as below.

The first step is to initialize the swarm by randomly assigning velocity and position to each particle in the search space. Then, the velocity and position of each particle are adjusted according to the information from its previous experience and neighbours in each iteration. Assume v_n^d and p_n^d denote the velocity and position of the nth particle in dth dimension. The velocity and position of each particle are updated as:

$$v_n^d = \omega * v_n^d + c1 * r_1^d * (PB_n^d - p_n^d) + c2 * r_2^d * (GB^d - p_n^d), \quad n = 1, 2, 3, \cdots, N; \quad d = 1, 2, 3, \cdots D \tag{50}$$

$$p_n^d = p_n^d + v_n^d, \quad j = 1, 2, 3, \cdots, J; \quad q = 1, 2, 3, \cdots Q \tag{51}$$

where ω represents the inertia weight, and r_1^d, r_2^d are two random numbers. In this paper, it is assumed that the value of ω is 0.6.[34] PB_n^d represents the best previous position of the nth particle in dth dimension, and its position is determined by the best fitness value Jp_n^d calculated from fitness function. Here, the mean square error is used as the cost function. The smallest value of Jp_n^d is recorded as Jg^d, and the corresponding best-so-far position is recorded as GB^d. The velocity and position of each particle cannot exceed the maximum value.

Results and discussion

Results

In light of the numerical study discussed in the "System description" section, unit delay block is used to implement in the discrete time case and the positive parameter d is calculated as:

$$d = \frac{Real\ distance}{Sound\ velocity} \times F_s \tag{52}$$

In this case, it is assumed that the microphone and the loudspeaker are the sources of nonlinearity, and they are modelled by a second-order Butterworth high-pass filter with a cut-off frequency 80 Hz.[33] A sampling frequency

Table 1. Number and corresponding distance ratio conditions.

1	$\lvert \frac{s_3}{s_4} > 1 > \frac{s_1}{s_2} \rvert$
2	$\lvert \frac{s_3}{s_4} > \frac{s_1}{s_2} > 1 \rvert$
3	$\lvert \frac{s_3}{s_4} = \frac{s_1}{s_2} > 1 \rvert$
4	$\lvert \frac{s_1}{s_2} > \frac{s_3}{s_4} > 1 \rvert$

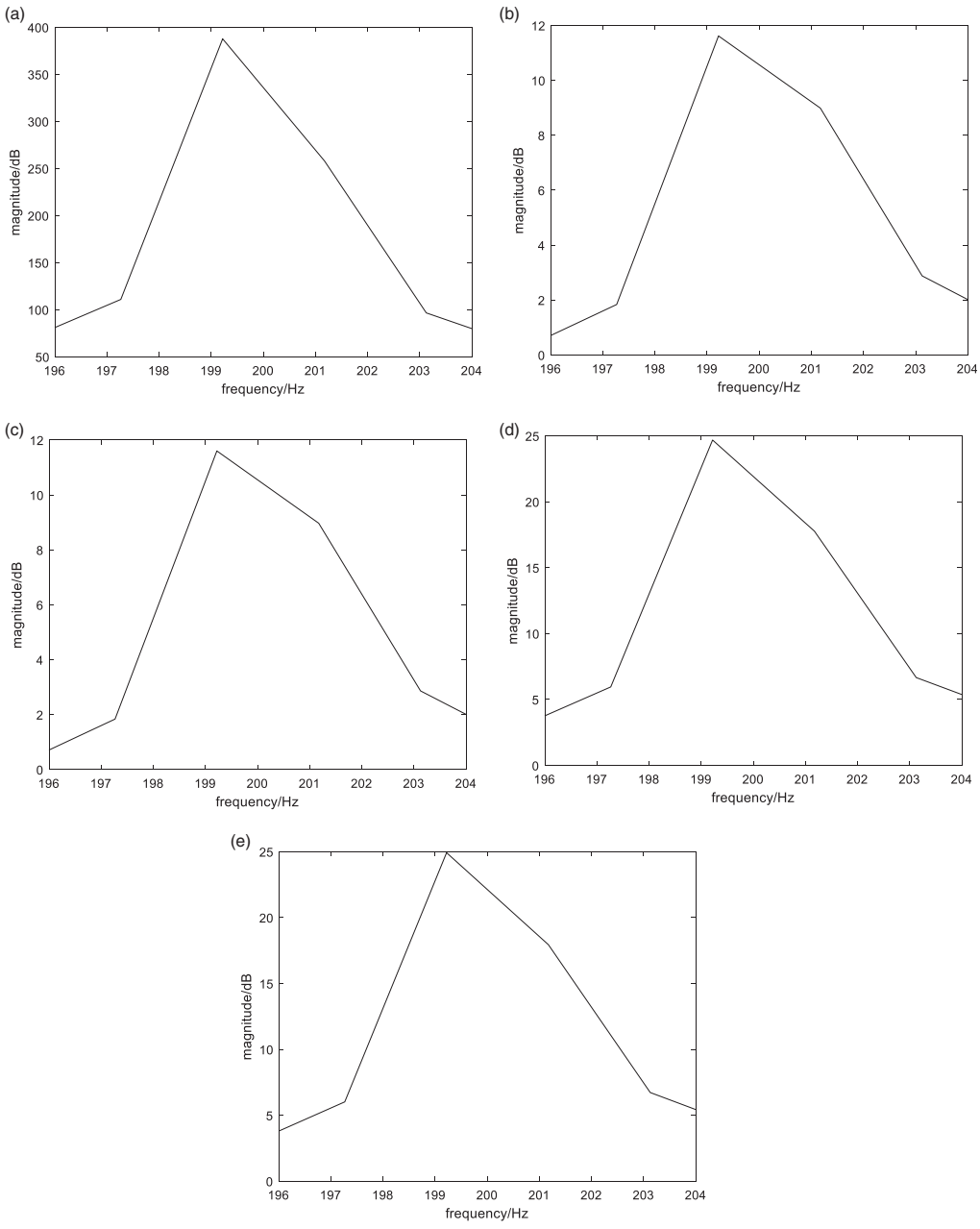

Figure 3. Cancellation performance of narrowband noise in frequency domain: (a) original noise, (b) first distance ratio, (c) second distance ratio, (d) third distance ratio and (e) fourth distance ratio.

Table 2. Magnitude of error signal of FIR filter and Volterra filter (for narrowband noise).

Name	$\lvert\frac{s_3}{s_4}\rvert > 1 > \lvert\frac{s_1}{s_2}\rvert$	$\lvert\frac{s_3}{s_4}\rvert > \lvert\frac{s_1}{s_2}\rvert > 1$	$\lvert\frac{s_3}{s_4}\rvert = \lvert\frac{s_1}{s_2}\rvert > 1$	$\lvert\frac{s_1}{s_2}\rvert > \lvert\frac{s_3}{s_4}\rvert > 1$
FIR filter	11.6 dB	11.7 dB	24.8 dB	25 dB
Volterra filter	11.6 dB	11.56 dB	24.6 dB	23.47 dB
Difference (FIR–Volterra)	+0 dB	+0.14 dB	+0.2 dB	+0.13 dB

FIR: finite impulse response.

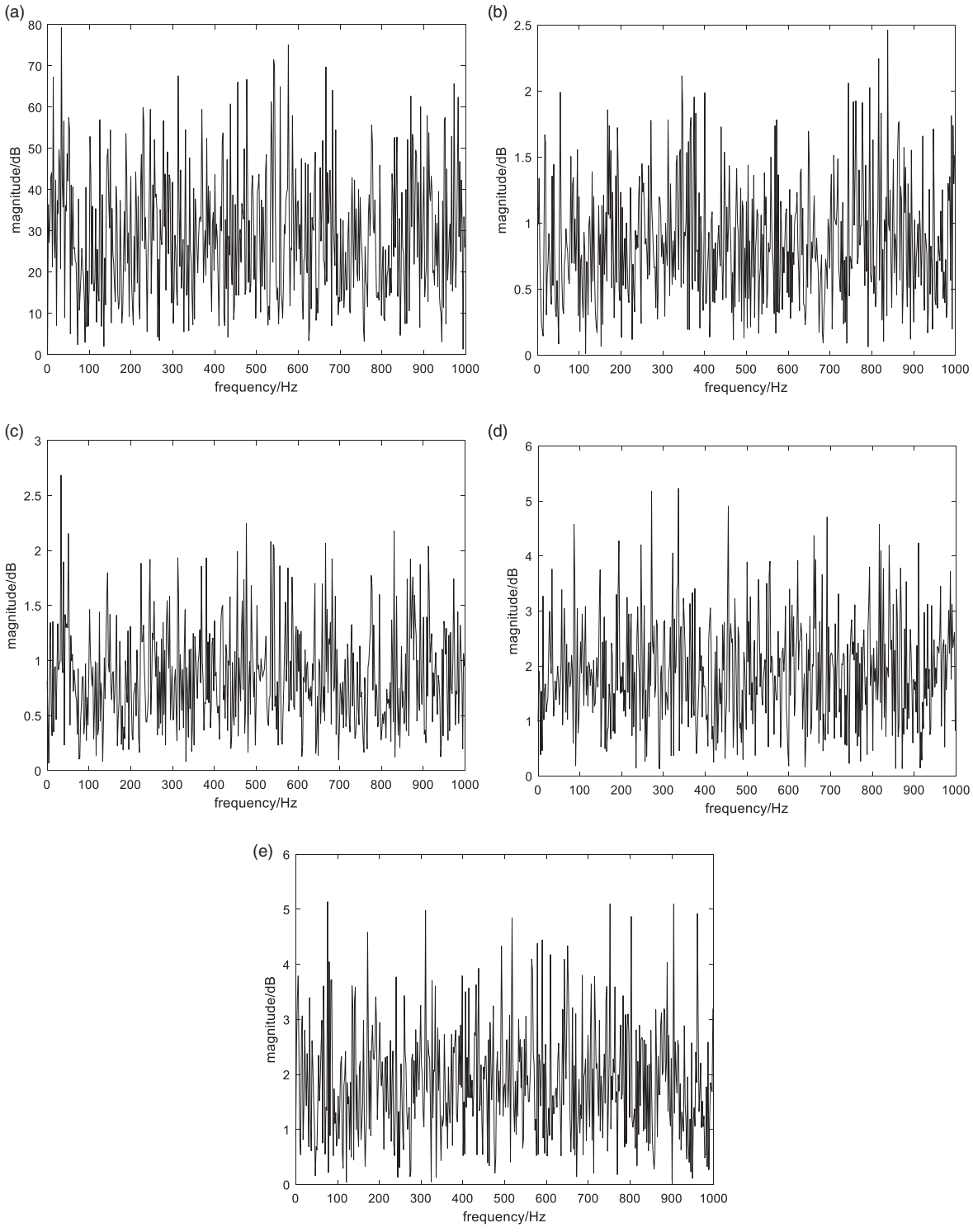

Figure 4. Cancellation performance for broadband noise: (a) original noise, (b) first distance ratio, (c) second distance ratio, (d) third distance ratio and (e) fourth distance ratio.

of 2000 Hz is used in all the simulations, and the memory length of the adaptive second-order Volterra filter is assumed 9, while the length of the coefficient vector of adaptive Volterra filter is 54.

All the simulations are developed in a free-field acoustic environment, and in order to precisely reflect the degree of cancellation, the error electrical signal is presented in the frequency domain; in the graphical results, the x label represents frequency in Hertz (Hz), and the y axis label denotes magnitude in decibels (dB).

Table 3. Average magnitude of error signal of FIR filter and Volterra filter (for broadband noise).

Name	$\lvert\frac{s_3}{s_4}\rvert > 1 > \lvert\frac{s_1}{s_2}\rvert$	$\lvert\frac{s_3}{s_4}\rvert > \lvert\frac{s_1}{s_2}\rvert > 1$	$\lvert\frac{s_3}{s_4}\rvert = \lvert\frac{s_1}{s_2}\rvert > 1$	$\lvert\frac{s_1}{s_2}\rvert > \lvert\frac{s_3}{s_4}\rvert > 1$
FIR filter	0.85 dB	0.86 dB	1.89 dB	1.85 dB
Volterra filter	0.8 dB	0.79 dB	0.8 dB	0.81 dB
Difference (FIR–Volterra)	+0.05 dB	+0.07 dB	+1.09 dB	+1.04 dB

FIR: finite impulse response.

Table 4. Comparison of computational complexity.

Name	Memory length	Multiplication	Addition
FIR filter	N	N	N
Volterra filter	N	N	$N(N+3)/2$

FIR: finite impulse response.

Case 1: Narrowband noise

In this simulation, a 200-Hz sine wave was selected as the narrowband noise to identify the cancellation capability and explore the effect of different distance ratios on the degree of cancellation. Table 1 presents the number and corresponding distance ratio condition, and Figure 3 shows the cancellation performance.

Case 2: Broadband noise

In this simulation, a Gaussian white noise with zero mean and unit variance was used as the primary noise and the distance in Table 1. The corresponding cancellation performance is shown in Figure 4.

Discussion

The simulation results in Figure 3 demonstrate the cancellation capability of the proposed ANC system for narrowband noise in the free-field acoustical environment. Figure 3(b) and (c) shows that the error electrical signal magnitude under the first and second distance ratio conditions was 11.6 dB and 11.7 dB, respectively while Figure 3(d) and (e) shows that the error magnitude under the third and fourth distance ratios was 24.6 dB and 23.47 dB, respectively. It is found that by increasing $\lvert\frac{s_1}{s_2}\rvert$, an average amount of 12 dB increment is presented in the presence of the magnitude of the error electrical signal, implying that the cancellation performance is degraded. In summary, the cancellation performance of the system with the narrowband noise indicates that the effect of different distance ratios on the cancellation performance is significant, and the cancellation performance of the narrowband noise is better when the value of $\lvert\frac{s_1}{s_2}\rvert$ is smaller than the value of $\lvert\frac{s_3}{s_4}\rvert$.

Table 2 presents a summary of comparison of the magnitude of the error signal of FIR filter-based[c] and Volterra filter-based ANC systems under different distance ratios. The memory length of the FIR filter was 9, same as of the Volterra filter. Relevant data about the cancellation performance of FIR filter-based ANC system can be found in the author's previously submitted paper.[28]

The results reveal that when compared to the FIR filter-based ANC system, for narrowband noise cancellation, the Volterra filter-based ANC system can achieve a small improvement.

The results in Figure 4 demonstrate the cancellation capability of the proposed ANC system for broadband noise. It is found that the maximum magnitude in Figure 4(d) and (e) was more than twice of the maximum magnitude in Figure 4(b) and (c), reflecting the significant effect of distance ratios. Besides, one can find that the optimal distance ratio configuration is that $\lvert\frac{s_3}{s_4}\rvert > 1 > \lvert\frac{s_1}{s_2}\rvert$, and the cancellation performance is degraded with the increase in $\lvert\frac{s_1}{s_2}\rvert$.

Table 3 presents the relevant comparison of cancellation performance for broadband noise in terms of average magnitude in dB.

From the comparison result, three characteristics are found. First, for Volterra filter-based ANC system, the difference in the average magnitude of the error signal was not big though the difference in the maximum magnitude was significant. Second, compared to the FIR filter-based ANC system, the Volterra filter-based ANC system could achieve some improvements andthe difference varied for different distance ratios. Third, the difference between performances of the Volterra-filter and the FIR-filter is increasing with the increment of $\lvert\frac{s_1}{s_2}\rvert$.

Table 4 presents a comparison of the computational complexity.

As noted above, with the value of $N = 9$ and the addition of Volterra filter is six times of the addition of FIR filter. Therefore, the computation load of the FIR filter is only 16.7% of the Volterra filter.

Conclusion

A physical configuration-based feedforward ANC structure with an adaptive SOV filter for cancellation of point source noise in three-dimensional linear propagation medium (free-field) has been presented. The inertia weight PSO algorithm has been employed in an adaptive control context. The relationship between the degree of cancellation and the distance has been presented, and a series of physical distance constraints have been proposed from a scalar value perspective. A 200-Hz periodic signal and Gaussian white noise have been used as the primary noise as candidates of narrowband and broadband noise to verify the cancellation capability of the proposed adaptive feedforward ANC system and assess the degree of cancellation under different distance ratios. Simulation results have shown that the effect of distance on the cancellation performance is significant, while the optimal condition is $|\frac{s_3}{s_4}| > |\frac{s_1}{s_2}|$, for both narrowband and broadband noise. Moreover, it has been shown that the cancellation performance degrades with increasing $|\frac{s_1}{s_2}|$, and this reveals that the detection sensor should be placed closer to the primary source. Furthermore, the Volterra filter-based ANC system can achieve some improvements in cancellation performance of narrowband noise and broadband noise with reasonable compromise with complexity.

Data Availability

Previously reported physical distance data were used to support this study, and this is available at https://journals.sagepub.com/doi/pdf/10.1260/026309208784425451. These prior studies (and datasets) are cited at relevant places within the text as references.[9–11] The average magnitude of the error electrical signal for FIR-filter-based ANC system has been obtained in the author's previously submitted paper.

Declaration of conflicting interests

The author(s) declared no potential conflicts of interest with respect to the research, authorship, and/or publication of this article.

Funding

The author(s) received no financial support for the research, authorship, and/or publication of this article.

Notes

a. Leitch and Tokhi[1] first proposed this concept.
b. Calculate the autocorrelation of a signal first and compute the Fourier transform.
c. Related data can be found in the author's previously submitted paper.

ORCID iD

Tongrui Peng https://orcid.org/0000-0003-4371-3281

References

1. Leitch RR and Tokhi MO. Active noise control systems. *IEE Proc A Phys Sci Meas Instrum Manage Educ Rev UK* 1987; 134: 525–546.
2. Kajikawa Y, Gan WS and Kuo SM. Recent advances on active noise control: open issues and innovative applications. *APSIPA Trans Signal Inf Process* 2012; 1: 1–21.
3. Peters RJ, Smith BJ and Hollins M. *Acoustics and noise control*. 3rd ed. London, UK: Pearson Education Limited, 2011, pp.34–53.
4. Nithin VG and Ganapati P. Advances in active noise control: A survey, with emphasis on recent nonlinear techniques. *Signal Process* 2013; 93: 363–377.
5. Kuo SM and Morgan DR. Active noise control: a tutorial review. *Proc IEEE* 1999; 87: 943–973.
6. Jiang JG and Li Y. Review of active noise control techniques with emphasis on sound quality enhancement. *Appl Acoust* 2018; 136: 139–148.

7. Lueg P. Process of silencing sound oscillations. Patent 2043416, USA, 1936.
8. Tokhi MO. *Design of active noise control systems with compact and distributed sources*. Research Report for the Department of Automatic Control and Systems Engineering. ACSE Research Report 533, August 1994. Department of Automatic Control and Systems Engineering, The University of Sheffield.
9. Raja Ahmad RK and Tokhi MO. Theoretical development of minimum effort active noise control with feedback inclusion architecture. *J Low Freq Noise Vib Active Control* 2008; 27: 75–81.
10. Raja Ahmad RK and Tokhi MO. Design of self-tuning minimum effort active noise control with feedback inclusion architecture. *J Low Freq Noise Vib Active Control* 2009; 28: 205–215.
11. Raja Ahmad RK and Tokhi MO. Analysis of geometry related constraints of minimum effort active noise control system. *J Low Freq Noise Vib Active Control* 2010; 29: 111–128.
12. Martin T and Roure A. Optimization of an active noise control system using spherical harmonics expansion of the primary field. *J Sound Vib* 1997; 201: 577–593.
13. Martin T and Roure A. Active noise control of acoustic sources using spherical harmonics expansion and a genetic algorithm: simulation and experiment. *J Sound Vib* 1998; 212: 511–523.
14. Duke CR, Sommerfeldt SD, Gee KL, et al. Optimization of control source locations in free-field active noise control using a genetic algorithm. *Noise Control Eng J* 2009; 57: 221–231.
15. Wrona S, Diego MD and Pawelczyk M. Shaping zones of quiet in a large enclosure generated by an active noise control system. *Control Eng Pract* 2018; 80: 1–16.
16. Kuo SM, Wu HT, Chen FK, et al. Saturation effects in active noise control systems. *IEEE Trans Circuits Syst I* 2004; 51: 1163–1171.
17. Kuo SM and Wu HT. Nonlinear adaptive bilinear filters for active noise control systems. *IEEE Trans Circuits Syst* 2005; 52: 617–624.
18. Sahib MA and Kamil R. Comparison of performance and computational complexity of nonlinear active noise control algorithms. *ISRN Mech Eng* 2011; 2011: 1–9.
19. Cheng CM, Peng ZK, Zhang WM, et al. Volterra-series-based nonlinear system modeling and its engineering applications: a state-of-the-art review. *Mech Syst Signal Process* 2017; 87: 340–364.
20. Tan LZ and Jiang J. Filtered-X second-order Volterra adaptive algorithms. *Electron Lett* 1997; 33: 671–672.
21. Tan L and Jiang J. Adaptive Volterra filters for active control of nonlinear noise processes. *IEEE Trans Signal Process* 2001; 49: 1667–1676.
22. Alberto C and Giovanni LS. Filtered-X affine projection algorithms for active noise control using Volterra filters. *EURASIP J Adv Signal Process* 2004; 12: 1841–1848.
23. Karaboga D and Akay B. A comparative study of Artificial Bee Colony algorithm. *Appl Math Comput* 2009; 214: 108–132.
24. Yim KH, Kim JB, Lee TP, et al. Genetic adaptive IIR filtering algorithm for active noise control. *Proc IEEE Int Fuzzy Syst Conf* 1999; 3: 1723–1728.
25. Russo F and Sicuranza GL. Accuracy and performance evaluation in the genetic optimization of nonlinear systems for active noise control. *IEEE Trans Instrum Meas* 2007; 56: 1443–1450.
26. Kennedy J and Eberhart RC. Particle Swarm Optimization. *Proc. IEEE International Conference on Neural Networks* 1995; 4: 1942–1948.
27. Rout NK, Das DP and Panda G. Particle swarm optimization based active noise control algorithm without secondary path identification. *IEEE Trans Instrum Meas* 2012; 61: 554–563.
28. Peng TR, Zhu QM, Tokhi MO, et al. Fuzzy logic feedforward active noise control with distance ratio and acoustic feedback using Takagi–Sugeon–Kang inference. *J Low Freq Noise Vib Active Control* 2019; 0: 1–16.
29. Kennedy J and Eberhart RC. Particle swarm optimization. *Proc IEEE Int Conf Neural Netw* 1995; 1: 1942–1948.
30. Everest FA. *Master handbook of acoustics*. 6th ed. New York, NY: McGraw-Hill Education TAB, 2014, pp.33–38.
31. Nelson PA and Elliott SJ. *Active control of sound*. London, UK: Academic Press Limited, 1992.
32. Johan AK. *Adaptive control*. 2nd ed. Boston, MA: Addison Wesley, 1995, pp.1–33.
33. Zhang QZ and Gan WS. Active noise control using a simplified fuzzy neural network. *J Sound Vib* 2004; 272: 437–449.
34. Shi Y and Eberhart R. A modified particle swarm optimizer. In: *Proceedings of the 1998 IEEE international conference on evolutionary computation and IEEE world congress on computational intelligence*, 4–9 May 1998, Anchorage, AK, pp.69–73.